Knot physics: Deriving the fine structure constant.

C. Ellgen*

(Dated: September 21, 2015)

Abstract

Knot physics describes the geometry of particles and fields. In a previous paper we described the topology and geometry of an electron. From the geometry of an electron we can construct a mathematical model relating its charge to its spin angular momentum. From experimental data, the spin angular momentum is $\hbar/2$. Therefore the mathematical model provides a comparison of electron charge to Planck's constant, which gives the fine structure constant α. We find that using only electromagnetic momentum to derive the fine structure constant predicts a value for α^{-1} that is about two orders of magnitude too small. However, the equations of knot physics imply that the electromagnetic field cusp must be compensated by a geometric field cusp. The geometric cusp is the source of a geometric field. The geometric field has momentum that is significantly larger than the momentum from the electromagnetic field. The angular momentum of the two fields together predicts a fine structure constant of $\alpha^{-1} \approx 136.85$. Compared to the actual value of $\alpha^{-1} \approx 137.04$, the error is 0.13%. Including the effects of virtual particles may reduce the error further.

*Electronic address: cellgen@gmail.com; www.knotphysics.net

This paper may receive additional updates for clarity.

I. BACKGROUND

This paper will use the assumptions from the paper "Knot physics: Spacetime in co-dimension 2" [1] (available at **www.knotphysics.net**), which is necessary background reading. Many mathematical conventions and assumptions will be carried over from that paper. The application of partial derivatives on embedded manifolds, in particular, may be unfamiliar to many readers. Mathematica™ documents are also available at **knotphysics.net** that provide mathematical modeling associated with the calculations here.

II. OVERVIEW

A. The fine structure constant

The fine structure constant is a dimensionless number α defined by the relation $\alpha = q^2/(4\pi\epsilon_0\hbar c)$ where q is the charge of the electron. In our discussion and calculations we will use $\epsilon_0 = \mu_0 = c = 1$. Then

$$\alpha = \frac{q^2}{4\pi\hbar} \tag{1}$$

The charge of the electron is the fundamental unit of charge associated with every elementary particle. Planck's constant is a unit of action that appears in a wide variety of quantum applications. The fact that the charge of every electron is the same and that every elementary particle has a charge which is an integer multiple of electron charge is of great physical significance, but derivation of that fact is not obvious. Furthermore, the number α that determines the magnitude of the elementary charge has not previously been shown to have a numerical formula in terms of non-physical constants. There is a very precise experimental measurement of α, but there is no known theoretical calculation that produces the number without experimental data as an input. The purpose of this paper is to show two things. First, we show that the properties of elementary fermions in knot physics imply leptons have unit charge. Second, we approximate the fine structure constant by applying those properties. Showing integer charge for hadrons and deriving an exact number for α are subjects for future work.

B. Running of the coupling

Experimental measurements of the fine structure constant show that its value depends on the energy scale of the measurement. In [1] we derive the Lagrangian from the fundamental assumptions and find that the electromagnetic component of the Lagrangian can be approximated as $\mathcal{L} = (1/2)wF^{\alpha\beta}F_{\alpha\beta}$, where $F^{\alpha\beta}$ is the electromagnetic field tensor. We see the familiar term $F^{\alpha\beta}F_{\alpha\beta}$, but we note that this Lagrangian is only a leading order approximation. In particular, we show that the electromagnetic field can reach infinite energy even while the tensor $F^{\alpha\beta}$ remains finite. Calculation of the running of the coupling would require including higher order terms in the Lagrangian. In this paper, we use only the leading order approximation and therefore neglect the running of the coupling.

C. Planck's constant

Planck's constant is a unit of action that appears in several different quantum calculations. Though it is not necessary for the purposes of this paper, it may help illuminate the calculation to hypothesize an interpretation of Planck's constant.

The spacetime manifold M has metric $g_{\mu\nu} = \rho^2 A_{\alpha,\mu}A^{\alpha}_{\ ,\nu}$. Using that metric, the manifold M is Ricci flat, $\hat{R}^{\mu\nu} = 0$. Even with that constraint, M has degrees of freedom such that the manifold is under-constrained. Therefore, the manifold maximizes entropy. In classical thermodynamics, a system at equilibrium averages $(1/2)kT$ of energy for each degree of freedom. Similarly, we hypothesize that the spacetime manifold M averages an amount of action $\hbar$ for each degree of freedom. Then M is a branched manifold such that for each degree of freedom the branches are randomly distributed with variance corresponding to Planck's constant. For an elementary fermion, the branches of M separate into branches with spin up and branches with spin down. The difference in angular momentum between spin up and spin down is a degree of freedom, therefore the difference in angular momentum is $\hbar$ and each spin orientation has average angular momentum of $\hbar/2$.

Regardless of the interpretation, it is known from experimental data that elementary fermions have spin angular momentum $S = \hbar/2$. We will derive a formula for spin angular momentum as a function of charge squared, $S(q^2) = \hbar/2$. This formula gives a comparison between charge and Planck's constant. We can therefore use it to find a value for the fine

structure constant as

$$\alpha^{-1} = \frac{4\pi\hbar}{q^2} = \frac{8\pi S(q^2)}{q^2} \tag{2}$$

where we have chosen to invert the equation to solve for α^{-1}.

D. Overview of the derivation

We derive the fine structure constant by deriving the electron's spin angular momentum as a function of charge. The electron has an electromagnetic field that comes to a cusp. Ricci flatness implies that an electromagnetic field cusp requires a corresponding geometric cusp to preserve flatness. The geometric cusp produces a geometric field that is proportional to the electromagnetic field. To find the momentum from the geometric field, we compare the energy in the geometric field to the energy in the electromagnetic field. The comparison is analogous to Hooke's law $E = (1/2)kx^2$. The electromagnetic field $F^{\mu\nu}$ has the analog of a spring constant k_F and spring extension x_F. The geometric field $C^{\mu\nu}$ has the analog of a spring constant k_C and spring extension x_C. We find that the geometric field extension is larger than the electromagnetic field extension by a factor of 4π, which means that $x_C = 4\pi x_F$. The spring constant for each field is proportional to the number of degrees of freedom in each field. The electromagnetic field is sensitive to the change of A^ν parallel to the manifold, which has 4 dimensions. The electromagnetic field therefore has 4 degrees of freedom. The geometric field is sensitive to the change of A^ν in 5 spatial dimensions, for 5 degrees of freedom. Therefore $k_C = (5/4)k_F$. We can then compare the energies and find that

$$E_C = (1/2)k_C x_C^2 = (1/2)(5/4)k_F(4\pi x_F)^2 = (20\pi^2)(1/2)k_F x_F^2 = 20\pi^2 E_F \tag{3}$$

The energy-momentum tensors of the two fields are proportional to each other, and therefore the energy and momentum in the geometric field is $20\pi^2$ times larger than the energy and momentum in the electromagnetic field. The total angular momentum is the sum of the contributions from the geometric and electromagnetic components. From that angular momentum, we solve for the fine structure constant. The result is $\alpha_{calc}^{-1} \approx 136.85$ with 0.13% error compared to the experimental measurement $\alpha_{exp}^{-1} \approx 137.04$. Virtual particles may have differing effect on the electromagnetic field energy compared to the geometric field energy, which may contribute error. These errors can be reduced by the calculation of additional Feynman diagrams.

III. COORDINATES

We will use the following three coordinate systems to describe particle geometry.

A. Cylindrical coordinates

The full 6 dimensions of the Minkowski space can be expressed as $(t, r, z, \phi, x^4, x^5)$ using notation that borrows from two different coordinate conventions. These coordinates will typically be used to describe fields and geometry when t, x^4, and x^5 are suppressed. In that case the coordinates are (r, z, ϕ).

B. Toroidal coordinates

$\mathbb{R}^3$ has toroidal coordinates (τ, σ, ϕ) that relate to polar coordinates (r, z, ϕ) as follows:

$$r = a\frac{\sinh\tau}{\cosh\tau - \cos\sigma}$$
$$z = a\frac{\sin\sigma}{\cosh\tau - \cos\sigma} \tag{4}$$

The sets of constant τ are tori centered around a circle of radius a. At distance zero from the circle we have $\tau = \infty$. At infinite distance from the circle we have $\tau = 0$. The sets of constant σ are spheres such that their intersection with sets of constant τ are orthogonal. Close to the circle, the coordinate σ is a polar angle around the circle. Toroidal coordinates are an orthogonal coordinate system. Their properties assist with field equations. We see sets of constant τ and σ illustrated in Fig. 1.

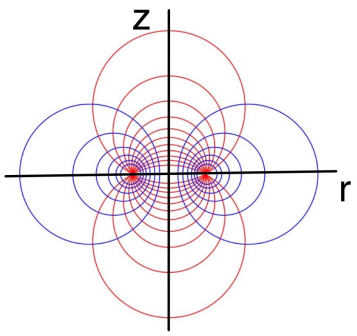

FIG. 1: This is a diagram of bipolar coordinates. The diagram shows sets of constant τ in blue and sets of constant σ in red in the rz plane. The value of τ increases to infinity as the size of the blue circles goes to zero. We extend to 3-dimensional toroidal coordinates by including the polar angle ϕ that has the same form as the polar angle of cylindrical coordinates.

C. Mapping coordinates

We use a map from 3 dimensions to 5 dimensions to describe an elementary fermion $\mathbb{R}^3\#(S^1 \times P^2)$. The coordinates of the 3-space are toroidal coordinates (τ, σ, ϕ) and the coordinates of the 5-space are a mix of toroidal and Cartesian coordinates $(\tau, \sigma, \phi, x^4, x^5)$. If we denote by T the solid torus $\tau > 1$, then we can map from $\mathbb{R}^3 - T$ to $\mathbb{R}^5$.

$$X(\tau, \sigma, \phi) = \Big(\tau/(1-\tau), \sigma, \phi, \tau \sin(2\sigma), \tau \cos(2\sigma)\Big) \tag{5}$$

The domain of the map is $\mathbb{R}^3 - T$, which is $\mathbb{R}^3$ with the solid torus T removed, where $\tau > 1$. Then it stretches $\mathbb{R}^3 - T$ to cover the missing torus using $\tau \to \tau/(1-\tau)$, so that points on the surface of the torus ($\tau = 1$) map to the circle at the center of the torus ($\tau = \infty$). Not only that, the map makes each point on the boundary of T identical to the point that is diametrically opposite it. This happens because we have

$$\begin{aligned} X(1, \sigma + \pi, \phi) &= (\infty, \sigma + \pi, \phi, \sin(2\sigma + 2\pi), \cos(2\sigma + 2\pi)) \\ &= (\infty, \sigma, \phi, \sin(2\sigma), \cos(2\sigma)) \\ &= X(1, \sigma, \phi) \end{aligned} \tag{6}$$

We see this illustrated in Fig. 2. The map X produces a knot $\mathbb{R}^3\#(S^1 \times P^2)$.

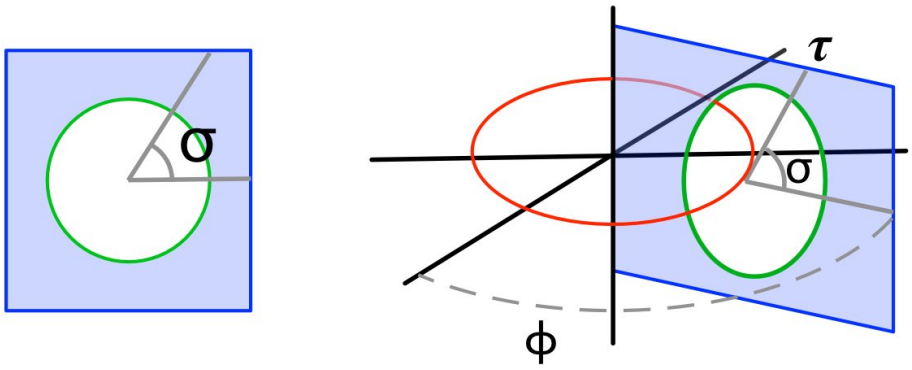

FIG. 2: On the left is $\mathbb{R}^2 - D^2$ with polar angle σ. On the right is $\mathbb{R}^3 - T$, in toroidal coordinates, with a slice at $\phi = \phi_0$. At the green circle we have $\tau = 1$. The map X makes opposite points on the circumference of the green circle identical. This identification of diametrically opposite points creates the topology $\mathbb{R}^2\#P^2$ in the left diagram and the topology $\mathbb{R}^3\#(S^1 \times P^2)$ in the right diagram.

IV. ELECTRON GEOMETRY

In this paper we will model the geometry, field, and angular momentum of a single electron that is at rest at infinite distance from any other particle. More specifcally, we will model a single branch of the branched manifold M. On that branch there is one knot that has the electron topology. Using its topology, we will derive geometric and physical characteristics of the knot. To simplify the description, we will make a few assumptions that are equivalent to the fixing the gauge, reference frame, and quantum branch weight of the branch that we are describing.

We fix the gauge by assuming that the field A^ν has the form $A^\nu = x^\nu + \varepsilon^\nu$ such that ε^ν goes to zero at infinite distance from the particle. We have the metric $g_{\mu\nu} = \rho^2 A_{\alpha,\mu} A^\alpha_{\ ,\nu}$. If $A^\nu = x^\nu$ then $g_{\mu\nu} = \rho^2 \bar{\eta}_{\mu\nu}$ where $\bar{\eta}_{\mu\nu}$ is the inherited metric using distances from the 6-space. Assuming $A^\nu = x^\nu + \varepsilon^\nu$ we have $g_{\mu\nu} = \rho^2(\bar{\eta}_{\mu\nu} + \epsilon_{\mu\nu})$ for some $\epsilon_{\mu\nu}$. We assume that the field is weak relative to its maximum possible value, and therefore we assume that $\epsilon_{\mu\nu}$ is small.

We fix the reference frame by assuming that the electron knot is at rest with its center at the origin of the 6-dimensional spatial coordinates $(t, 0, 0, 0, 0, 0)$.

We fix the quantum branch weight of the branch we are describing by assuming that the weight w goes to 1 at infinite distance from the electron knot. This also implies that ρ goes to 1 because $w = \rho^4$.

A. Ricci flatness with no electromagnetic field

1. *Flatness in 2 dimensions*

We begin by finding Ricci flat solutions for $\mathbb{R}^2 \# P^2$, the 2-dimensional case. To make $\mathbb{R}^2 \# P^2$ we remove a disk from a plane and set each point on the disk boundary identical to the point that is diametrically opposite. Although the disk with the plane removed, $\mathbb{R}^2 - D^2$, is flat, when we identify points to create $\mathbb{R}^2 \# P^2$, it is no longer flat unless we meet certain conditions for ρ. We draw a circle on the manifold around the P^2 as in the left diagram of Fig. 3. We cut along the circle to produce a manifold with boundary, which we call M_2, as in the middle diagram of Fig. 3. Then we apply the Gauss-Bonnet theorem to M_2,

$$\int_{M_2} \hat{R}\, \mathrm{d}A + \int_{\partial M_2} k_g\, \mathrm{d}s = 2\pi\chi(M_2) \tag{7}$$

In this equation, the symbols are the conventional ones for this theorem. The geodesic curvature k_g provides a measure of how much a curve deviates from a geodesic in a manifold, and the Euler characteristic χ depends only on the topology of the manifold. We have $\hat{R} = 0$ on M_2. The Euler characteristic of P^2 is $\chi(P^2) = 1$. The Euler characteristic of M_2 (equivalent to $P^2 - D^2$) is $\chi(M_2) = 0$. The geodesic curvature is $k_g = 0$ at every radius. Zero geodesic curvature requires that perpendicular lines passing through the circles do not diverge relative to $g_{\mu\nu}$. We conclude that the red lines in the right diagram of Fig. 3 span an equal length on each circle. Therefore, on a flat $\mathbb{R}^2 \# P^2$ the circumference is constant at every radius, as illustrated in the right diagram of Fig. 3. The manifold has the same geometry as a cylinder. We can use a parameter $a = \xi e^{i\theta}$ to describe the geometry. If we consider M_2 as an embedding, in the same sense as the mapping that we used for $\mathbb{R}^3 \#(S^1 \times P^2)$, which was

$$X(a; \tau, \sigma, \phi) = \Big(\tau/(1-\tau), \sigma, \phi, \xi\tau \sin(2\sigma + \theta), \xi\tau \cos(2\sigma + \theta)\Big) \tag{8}$$

then we can describe the geometry of M_2 in terms of the magnitude ξ. In the degenerate case that the magnitude ξ goes to zero, M_2 approaches a flat disk and the weight ρ compensates the geometry such that $C\rho = b$ for circumference C and constant b. In the right diagram of Fig. 3 we see a $\mathbb{R}^2 \# P^2$ with a few circles shown as examples of circumferences around the P^2. Ricci flatness requires that those circles have constant circumference, with conformal weight ρ such that $\rho = b/C$.

We now consider a more general solution for Ricci flatness on $\mathbb{R}^2$. In 2 dimensions, for any harmonic function κ, if a metric $\bar{\eta}_{\mu\nu}$ is Ricci flat then the metric $e^{2\kappa}\bar{\eta}_{\mu\nu}$ is also Ricci flat [3]. In our case we start with Ricci flat $\bar{\eta}_{\mu\nu}$ and we construct harmonic function κ. For multiple source points p_i there is a harmonic function $\kappa(x) = \sum_i -\ln(d(p_i, x))$ where $d(p_i, x)$ is the distance from p_i to x. Then $\rho = e^{\kappa}$ and $\rho^2\bar{\eta}_{\mu\nu}$ is a Ricci flat metric. If there is only one source, this solution exactly matches the solution we obtained before for the degenerate P^2, which was $\rho = e^{\kappa} = 1/d = b/C$. Thus we can replace the points p_i by a degenerate P^2 (one for which its embedding has magnitude $\xi = 0$). If the magnitude ξ increases, then the displacement of the embedding into x^4 and x^5 increases, which increases the length of a path around the P^2. Therefore, increasing the magnitude ξ increases the circumference C. Ricci flatness requires that the weighted circumference $C\rho$ is constant, therefore ρ changes to preserve the weighted circumference $C\rho$.

Next let us consider the case of $\mathbb{R}^2$ with natural metric $\bar{\eta}_{\mu\nu} = \text{diag}(1, 1)$. Later we will

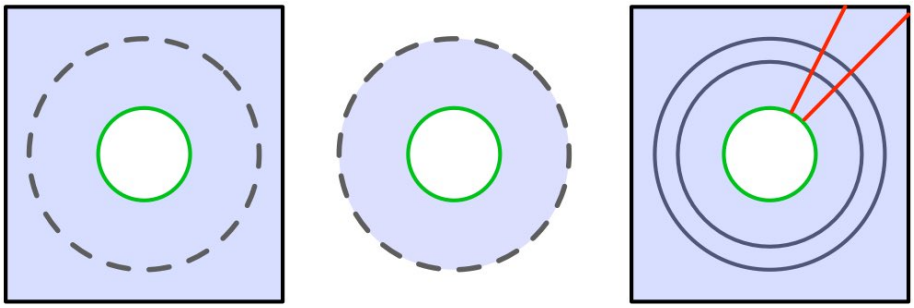

FIG. 3: In the left diagram, we see a $\mathbb{R}^2 \# P^2$ with a circle drawn around it. We cut on the circle to produce the manifold M_2, as shown in the middle diagram. If $\hat{R} = 0$ on the interior of M_2, then, by the Gauss-Bonnet theorem, the geodesic curvature on the boundary of M_2 is $k_g = 0$. This is true for any circular boundary we draw. For example, in the right diagram we see some examples of circular boundaries on which the geodesic curvature is zero. Zero geodesic curvature requires that perpendicular lines passing through the circles do not diverge relative to $g_{\mu\nu}$. For example, the red lines shown do not diverge. We conclude that the red lines span an equal length on each circle. Therefore any such circle has constant circumference relative to $g_{\mu\nu}$, with conformal weight ρ such that $C\rho = b$.

use this plane as the slice $\phi = 0, \phi = \pi$ through $\mathbb{R}^3 \# (S^1 \times P^2)$, but we completely suppress the third dimension for the moment. In this slice let us assume there is a P^2 with $\xi = 0$ at the point $p_1 = (1, 0)$ and at the point $p_2 = (-1, 0)$, as in the left diagram of Fig. 4. We begin by finding the harmonic function $\kappa(x) = \sum_i -\ln(d(p_i, x))$ and then $\rho = e^{\kappa}$. Now we use the metric $\rho^2 \bar{\eta}_{\mu\nu}$ with degenerate P^2 at each of the points p_i. In the right diagram of Fig. 4 we see bipolar coordinates, which are the 2-dimensional version of toroidal coordinates with ϕ angle suppressed. The circles in blue are the same as the circles of constant τ in toroidal coordinates. Relative to $\rho^2 \bar{\eta}_{\mu\nu}$, these circles have constant circumference $C\rho$. We can increase the magnitude ξ of both of the P^2 as desired, compensating for the geometry by reducing ρ as needed. Bipolar coordinates give an isometric mapping between the cylinder $\mathbb{R} \times S^1$ and the Ricci flat $\mathbb{R}^2 \# P^2 \# P^2$. The blue circles of Fig. 4 are mapped from the circles of the cylinder corresponding to the S^1 fiber. The red circles of Fig. 4 are mapped from the parallel lines of the cylinder corresponding to the $\mathbb{R}$ fiber.

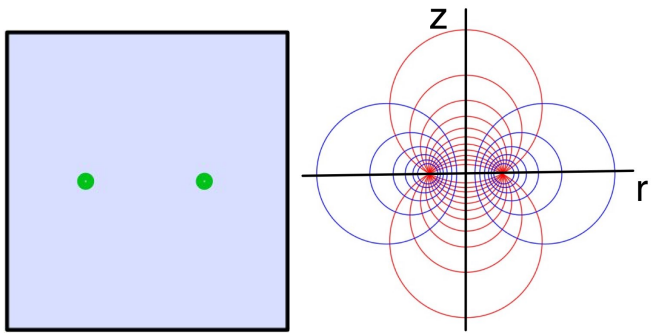

FIG. 4: We see a $\mathbb{R}^2\#P^2\#P^2$ with a P^2 at the point $p_1 = (1, 0)$ and at the point $p_2 = (-1, 0)$. We will later use this as a slice through a $\mathbb{R}^3\#(S^1 \times P^2)$. The diagram on the right shows bipolar coordinates centered around p_1 and p_2. Bipolar coordinates are the 2-dimensional version of toroidal coordinates with the ϕ coordinate suppressed. The circles of constant τ, shown in blue, have constant circumference relative to $\rho^2\bar{\eta}_{\mu\nu}$. The circles of constant σ, shown in red, are also geodesics relative to $\rho^2\bar{\eta}_{\mu\nu}$.

2. Flatness in 2+1 dimensions

Now we introduce the time dimension. The usual inherited metric for a flat manifold is $\bar{\eta}_{\mu\nu} = \text{diag}(1, -1, -1)$. Introducing the manifold $\mathbb{R} \times (\mathbb{R}^2\#P^2\#P^2)$, we have P^2 on the manifold at $p_1 = (t, 1, 0)$ and $p_2 = (t, -1, 0)$. We can scale the metric as above to get $\rho^2\bar{\eta}_{\mu\nu}$. The volume in 3 dimensions, however, scales by ρ^3, and we find that the time dimension makes the conformal scaling no longer Ricci flat. To compensate for the time dimension, we use symmetry and motion. Rather than beginning with initial metric $\bar{\eta}_{\mu\nu} = \text{diag}(1, -1, -1)$, we introduce an embedding of the manifold that is in motion with some velocity β. We set β such that $\gamma = \rho$. Then the inherited metric is $\bar{\eta}_{\mu\nu} = \text{diag}(1/\gamma^2, -1, -1) = \text{diag}(1/\rho^2, -1, -1)$. Thus the metric includes the factor $\rho(\Delta t/\gamma) = \Delta t$ and the metric becomes $\rho^2\bar{\eta}_{\mu\nu}$, which is Ricci flat.

In the previous section, we mapped isometrically to the manifold $\mathbb{R}^2\#P^2\#P^2$ from the cylinder $S^1 \times \mathbb{R}$. Here, we can map isometrically to this manifold $\mathbb{R} \times (\mathbb{R}^2\#P^2\#P^2)$ from $\mathbb{R} \times (\mathbb{R} \times S^1)$. The manifold $\mathbb{R} \times (\mathbb{R} \times S^1)$ with its natural metric is Ricci flat. Therefore this manifold with its embedding and conformal weight is also Ricci flat. Again, the magnitude ξ of the P^2 can be expanded and ρ is reduced to compensate. Now that ρ is linked to motion through $\rho = \gamma$, we see that reducing ρ reduces the velocity. In particular, a P^2 that is fully

expanded to $\rho = 1$ has no motion.

3. Flatness in 3+1 dimensions

Introducing the third spatial dimension, we again find that adjustments are necessary to produce Ricci flatness. The Weyl metric gives a description of any axially symmetric Ricci flat geometry in terms of two potential functions, U and V. In cylindrical coordinates (t, r, z, ϕ) the Weyl metric is

$$\mathrm{d}s^2 = e^{2U}\mathrm{d}t^2 - e^{-2U}(r^2\mathrm{d}\phi^2 + e^{2V}(\mathrm{d}r^2 + \mathrm{d}z^2)) \tag{9}$$

The potential function U satisfies the Laplacian

$$\nabla^2 U = U_{,zz} + U_{,rr} + (1/r)U_{,r} = 0 \tag{10}$$

and the potential function V is related in the following way

$$V_{,r} = r((U_{,r})^2 - (U_{,z})^2) \tag{11a}$$

$$V_{,z} = 2rU_{,r}U_{,z} \tag{11b}$$

We can extend the description that we used for 2+1 dimensions by saying that the harmonic function κ is analogous to the potential function U. For 3+1 dimensions, we use a harmonic function κ whose source is the degenerate $S^1 \times P^2$. The function κ is uniquely determined by its source, up to a constant factor. The function U, which also satisfies the Laplacian, is proportional to κ. Subsequently we can solve for V in terms of U.

Ideally we would solve for exact solutions U and V. Here, we will sketch a derivation of approximations for U and V. To derive an approximation, we consider a slice of $\mathbb{R}^4$ with constant t and constant ϕ, and we observe the behavior of U and V near the degenerate $S^1 \times P^2$ at $(r, z, \phi) = (1, 0, 0)$. Furthermore, we consider behavior only along the r coordinate, so that $z = 0$. In this case, we have

$$U = -\ln|r - 1| \tag{12a}$$

$$V_{,r} = r(U_{,r}))^2 = r\Big(\frac{\mathrm{d}}{\mathrm{d}r}(-\ln|r-1|)\Big)^2 \tag{12b}$$

In the limit of approaching the degenerate $S^1 \times P^2$, the radial term r is approximately constant in comparison to the derivatives. We therefore have

$$V_{,r} = (U_{,r})^2 = \Big(- \frac{\mathrm{d}}{\mathrm{dr}} \ln |r-1| \Big)^2 = \Big(\frac{2}{r-1} \Big)^2 \tag{13}$$

$$V = - \frac{4}{r-1} \tag{14}$$

We obtain the same result by performing the integral in eqn. (13) exactly and ignoring the smaller term near the $S^1 \times P^2$. Near the $S^1 \times P^2$, the effect of the function V dominates over that of $U = - \ln |r-1|$. Just inside the torus, two nearby points with slightly different r will have a large $\mathrm{d}s$ according to eqn. 9, since $r \lesssim 1$ and $V \gg 0$. Just outside the torus, two nearby points with slightly different r will have a small $\mathrm{d}s$ since $r \gtrsim 1$ and $V \ll 0$. As we go from the inside of the ring to the outside, the sign of V changes and we see that, in the limit as we approach the degenerate $S^1 \times P^2$, the average value of V is zero. The potential U has the correct asymptotic behavior for both the near case, as we approach the degenerate $S^1 \times P^2$, and the far case as we approach asymptotic flatness at infinite distance. In the near case, the spacelike components of the metric have conformal weight ρ that scales like $1/r$ and preserves Ricci flatness on the $S^1 \times P^2$ in the same way as the two dimensional case. In the far case, the spacelike components of the metric have conformal weight ρ that scales like $e^{1/r}$ in the same way as any compact source with flat background. We therefore take as an approximation that $V = 0$ everywhere and that we can obtain this approximation from the Weyl metric by a coordinate transformation. (See [2] for some discussion of such a coordinate transformation.) We therefore arrive at the conformastatic metric

$$\mathrm{d}s^2 = e^{-2\kappa} \mathrm{d}t^2 - e^{2\kappa} (r^2 \mathrm{d}\phi^2 + \mathrm{d}r^2 + \mathrm{d}z^2) \tag{15}$$

such that κ is a harmonic function, where we note that κ is proportional to any harmonic function U whose source is the degenerate $S^1 \times P^2$.

In the previous section we had the problem that introducing the time dimension added a factor ρ to the volume element, and we dealt with that problem by adding motion to the embedding. Here we are introducing the ϕ dimension, and this adds another factor ρ to the volume element. The volume element of the manifold is $\mathrm{d}V/\gamma$, and therefore if the manifold M is oriented such that $\gamma = \rho^2$, then a factor γ will compensate for the factors of ρ in both the t and ϕ coordinate. By comparison, in the 2+1 case, the conformal weight scales $\mathrm{d}t^2$ by

ρ^2 and the embedding introduces a factor $\gamma = \rho$, so that we have

$$\rho^2\Big(\frac{\mathrm{d}t}{\gamma}\Big) = \rho^2\Big(\frac{1}{\rho^2}\Big)\mathrm{d}t^2 = \mathrm{d}t^2 \tag{16}$$

In the 3+1 case, the $\mathrm{d}t^2$ term scales by ρ^2 and the embedding introduces a factor $\gamma = \rho^2$, so that we have

$$\rho^2\Big(\frac{1}{\rho^4}\Big)\mathrm{d}t^2 = \Big(\frac{1}{\rho^2}\Big)\mathrm{d}t^2 = e^{-2\kappa}\mathrm{d}t^2 \tag{17}$$

Again, the P^2 geometry can be expanded, and ρ compensates such that circumference is conserved. Likewise, as ρ reduces, $\gamma = \rho^2$ implies that the velocity of motion also reduces.

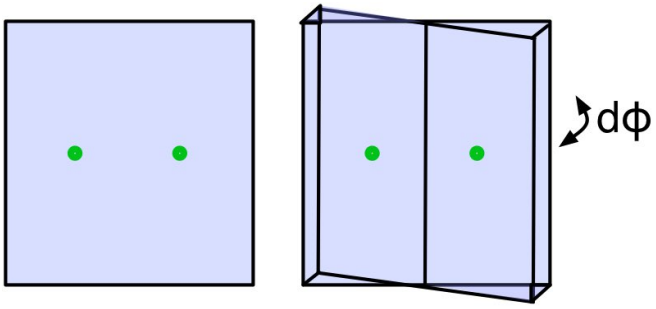

FIG. 5: On the left is $\mathbb{R}^2$ with degenerate P^2 at $(r, z, \phi) = (1, 0, 0)$ and $(r, z, \phi) = (1, 0, \pi)$. The harmonic function κ is $\kappa(x) = \sum_i -\ln(d(p_i, x))$. On the right is a $d\phi$ slice from $\mathbb{R}^3$ with corresponding harmonic function κ that is weighted by $r\mathrm{d}\phi$. The dots indicate the location of the degenerate $S^1 \times P^2$ in this $\mathrm{d}\phi$ slice.

We call the distance from a point to the particle d. In three spatial dimensions, far away from a particle κ scales as $1/d$. Therefore $\lim_{d\to\infty} e^{\kappa} = \lim_{d\to\infty} e^{1/d} = 1$. This is in contrast to the 2-dimensional solution where κ scales like $-\ln(d)$, and ρ converges to zero at infinite distance. Therefore, in three dimensions it makes sense to say that at infinite distance $\rho = 1$ and $\gamma = \rho^2 = 1$.

B. Ricci flatness with weak field

In this section we will use the coordinate convention

$$(y^0, y^1, y^2, y^3, y^4, y^5) = (t, r, z, \phi, x^4, x^5) \tag{18}$$

so that we can use numerical indices $1, 2, 3$ to represent cylindrical coordinates. This provides an index $y^3 = \phi$ that runs parallel to the S^1 fiber of the knot.

The electromagnetic field $F^{\mu\nu}$ on the electron comes to its maximum at a cusp. Using the map $X(\tau, \sigma, \phi)$, the cusp occurs at $X(1, \sigma, \phi)$, as in Fig. 6. Even at the cusp, the geometry must be Ricci flat. In local coordinates Ricci flatness can be written

$$\partial^\lambda \partial_\lambda g_{\mu\nu} = 0 \tag{19}$$

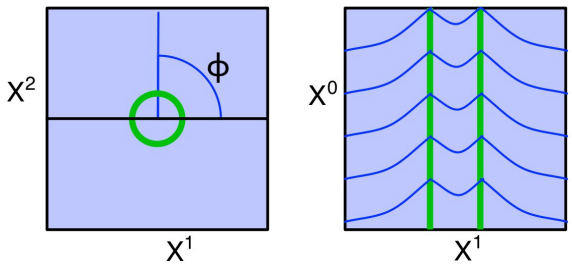

FIG. 6: In the left figure, we see a "top view" of a $\mathbb{R}^3 \# (S^1 \times P^2)$ with coordinates x^1 and x^2 as shown. The green circle represents the torus $X(1, \sigma, \phi)$ where X is the map associated with $\mathbb{R}^3 \# (S^1 \times P^2)$. Relative to the map X, the slice is at an angle of constant σ, and the angle ϕ is shown. The dark line is a constant x^2 slice that passes through the $\mathbb{R}^3 \# (S^1 \times P^2)$ at two points. We then show that slice in x^0 and x^1 coordinates. The blue curves are sets of constant A^0. The gradient of those lines is the electric field $A^0{}_{,\nu}$.

For the terms on the diagonal, g_{jj}, the Ricci flatness constraint in local coordinates is $\partial_\lambda \partial^\lambda g_{jj} = \partial_\lambda \partial^\lambda (A_{\alpha,j} A^\alpha{}_{,j}) = 0$ (no sum over j is implied). The electric field $A^0{}_{,j}$ comes to a cusp. To preserve the flatness constraint $\partial_\lambda \partial^\lambda (A_{\alpha,j} A^\alpha{}_{,j}) = 0$, the magnetic field satisfies $A^3{}_{,j} = A^0{}_{,j}$ in a neighborhood of the cusp so that the $A_{3,j} A^3{}_{,j}$ term negates the $A_{0,j} A^0{}_{,j}$ term. Then $F^{\alpha\beta} F_{\alpha\beta} = 0$ at the cusp. We can consider the electromagnetic field as if it has a charge current source J^ν. The relationship between $A^3{}_{,j}$ and $A^0{}_{,j}$ on the cusp implies a current J^ν with $J^0 = J^3 \neq 0$ and $J^1 = J^2 = 0$. Off the cusp, the current is zero, $J^\nu = 0$.

The electric field also affects the metric components $g_{0\nu} = \rho^2 A_{\alpha,0} A^{\alpha}{}_{,\nu}$. To preserve the constraint $\partial^\lambda \partial_\lambda g_{\mu\nu} = 0$, we have the geometric components of $g_{\mu\nu}$ compensate the electric field components. We can separate out the electric field component of the metric as

$$g_{0\nu} = \rho^2 A_{\alpha,0} A^{\alpha}{}_{,\nu} = \rho^2 (A_{0,0} A^{0}{}_{,\nu} + \sum_{\alpha \neq 0} A_{\alpha,0} A^{\alpha}{}_{,\nu}) \tag{20}$$

We have $A_{0,0} = 1$. The conformal weight ρ must be smooth at the cusp, otherwise the diagonal components of $g_{\mu\nu}$ would break Ricci flatness. Therefore the other terms of eqn. (20) have a cusp with $\partial_\lambda \partial^\lambda (\sum_{\alpha \neq 0} A_{\alpha,0} A^{\alpha}{}_{,\nu})$ equal to $-\partial_\lambda \partial^\lambda A^{0}{}_{,\nu}$, which implies the cusp has the same magnitude as the electric field cusp.

The magnetic field affects the metric components $g_{3\nu} = \rho^2 A_{\alpha,3} A^{\alpha}{}_{,\nu}$. We separate out the magnetic field component of the metric

$$g_{3\nu} = \rho^2 A_{\alpha,3} A^{\alpha}{}_{,\nu} = \rho^2 (A_{3,3} A^{3}{}_{,\nu} + \sum_{\alpha \neq 3} A_{\alpha,3} A^{\alpha}{}_{,\nu}) \tag{21}$$

We have $A_{3,3} = 1$. Therefore the other terms have a cusp with $\partial_\lambda \partial^\lambda (\sum_{\alpha \neq 3} A_{\alpha,0} A^{\alpha}{}_{,\nu})$ equal to $-\partial_\lambda \partial^\lambda A^{3}{}_{,\nu}$, which implies their cusp has the same magnitude as the magnetic field cusp.

We assumed that the electromagnetic field is weak such that the metric can be approximated as $g_{\mu\nu} = \rho^2(\bar{\eta}_{\mu\nu} + \epsilon_{\mu\nu})$, where $\epsilon_{\mu\nu}$ is a small contribution resulting from the electromagnetic field. From the previous discussion in this section, we see that Ricci flatness $\hat{R}^{\mu\nu} = 0$ requires that the metric $\bar{\eta}_{\mu\nu}$ must compensate the curvature of $\epsilon_{\mu\nu}$ at the electromagnetic field cusp. The metric $\bar{\eta}_{\mu\nu}$ is entirely geometric, it gives the distances in the embedding space. Therefore we are compensating an electromagnetic field with a geometric field. The only available variation of the geometry is waves in the x^4 and x^5 coordinates. We can describe these waves using the $\mathbb{R}^3 \# (S^1 \times P^2)$ map. If we include the time coordinate and the particle's quantum phase rotation (as in [1]), we have the map

$$X(t, \tau, \sigma, \phi) = \Big(t, \tau/(1-\tau), \sigma, \phi, \tau \sin(2\sigma + \omega t), \tau \cos(2\sigma + \omega t)\Big) \tag{22}$$

We note that the rotation resulting from ω does not produce waves at the cusp. The cusp is at $X(t, 1, \sigma, \phi)$ and this always maps to the unit circle in x^4 and x^5. This is the only part of the map that has no motion resulting from the ω rotation term. We will use a modification of eqn. (22) to achieve Ricci flatness. We modify the map with a function $h(t, \tau, \sigma, \phi)$ that changes the amplitude of the knot as a function of position. Then we have the map

$$X(t, \tau, \sigma, \phi) = \Big(t, \tau/(1-\tau), \sigma, \phi, h\tau \sin(2\sigma + \omega t), h\tau \cos(2\sigma + \omega t)\Big) \tag{23}$$

The value of h stays close to $h \approx 1$ and we use h to produce small waves that circulate around the particle, as in Fig. 7.

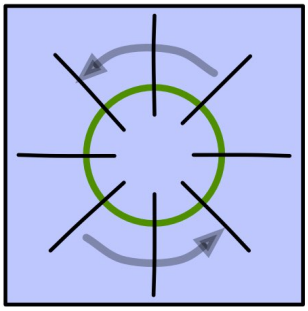

FIG. 7: A neutral $\mathbb{R}^3\#(S^1 \times P^2)$ with angular momentum has transverse waves that rotate around the particle. The transverse waves have periodic change in the x^4 and x^5 displacement. This is a top view slice through a $\mathbb{R}^3\#(S^1 \times P^2)$. The black lines are lines of constant phase in the x^4 and x^5 coordinates with rotation as indicated by the arrows.

The metric is $g_{\mu\nu} = \rho^2(\bar{\eta}_{\mu\nu} + \epsilon_{\mu\nu})$ and the geometric component is $\bar{\eta}_{\mu\nu}$. We recall our assumption that $A^\nu = x^\nu + \varepsilon^\nu$. The waves that circulate around the particle change the components A^4 and A^5 such that the derivatives $A_{4,0}$, $A_{5,0}$, $A^4{}_{,\nu}$, and $A^5{}_{,\nu}$ satisfy eqn. (20). Likewise, the geometric waves have derivatives $A_{4,3}$, $A_{5,3}$, $A^4{}_{,\nu}$, and $A^5{}_{,\nu}$ that satisfy eqn. (21). This implies that the waves produce a geometric cusp that matches, and is opposite to, the cusp of the electromagnetic field. To achieve that, we modify the function h so that the phase of the wave depends on position. The wave phase advances as a function of position so that the phase displacement comes to a cusp at the same location as the electromagnetic field. In the map of eqn. (23), the function h contributes to A^4 and A^5. The eqns. (20) and (21) show that the derivatives of h come to a cusp whose magnitude in time derivatives is determined by $\partial_\lambda\partial^\lambda(h^{,0}h_{,\nu}) = -\partial_\lambda\partial^\lambda(A^0{}_{,\nu})$ and whose magnitude in spatial derivatives is determined by $\partial_\lambda\partial^\lambda(h^{,3}h_{,\nu}) = -\partial_\lambda\partial^\lambda(A^3{}_{,\nu})$. This relates the magnitude of the geometric field cusp to the magnitude of the electromagnetic field cusp.

The waves on a charged knot advance in phase approaching the cusp, as in Fig. 8. In this way, the curvature of the electromagnetic field cusps in $A^0{}_{,\nu}$ and $A^3{}_{,\nu}$ is negated by the knot geometry to make the Ricci curvature flat at the cusp, $\partial^\lambda\partial_\lambda g_{\mu\nu} = 0$. In particular $\partial^\lambda\partial_\lambda g_{0\nu} = 0$ and $\partial^\lambda\partial_\lambda g_{3\nu} = 0$. See Fig. 9

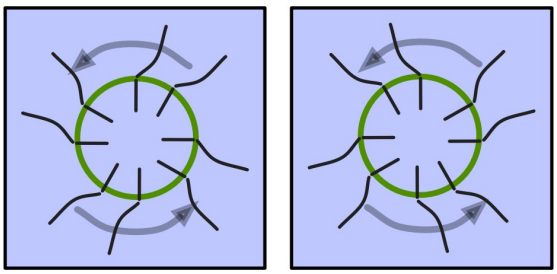

FIG. 8: If the $S^1 \times P^2$ is charged then the electromagnetic field comes to a cusp on the green circle. The cusp interferes with Ricci flatness. The geometry must compensate to restore $\hat{R}^{\mu\nu} = 0$. To do this, the rotating waves on the particle change phase based on the distance to the cusp. Depending on the sign of the particle charge, the phase either moves forward (as on the left) or backward (as on the right).

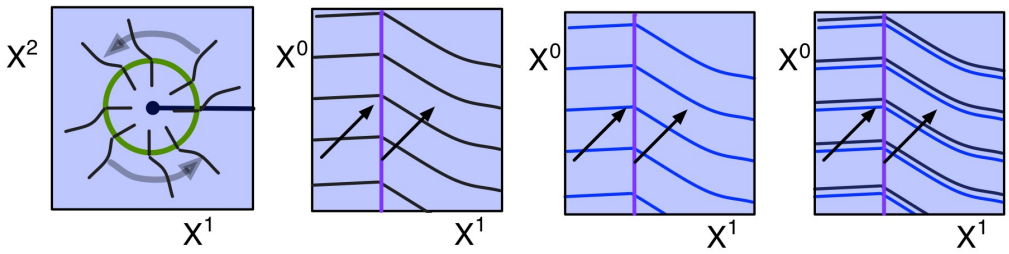

FIG. 9: In the left diagram we take a slice of the $\mathbb{R}^3 \# (S^1 \times P^2)$, in the x^1 direction (as indicated by the dark line) and the time dimension. In the second diagram, the black lines are lines of constant phase of the waves rotating around the particle. In the third diagram, the blue lines are lines of constant A^0 (as in Fig. 6). Crossing more black lines indicates traveling a greater distance, the path has greater change in x^4 and x^5. Crossing more blue lines indicates traveling a shorter distance by the metric $g_{\mu\nu} = \rho^2 A_{\alpha,\mu} A^{\alpha}{}_{,\nu}$ because change of A^0 reduces the effective distance traveled. The number of lines crossed by the arrows indicates the effect on $g_{0\nu}$. If only the electric field contributed to the metric, then $g_{0\nu}$ would change at the cusp in a way that would not be Ricci flat, (because $\partial_\lambda \partial^\lambda g_{0\nu} \neq 0$). To compensate, the geometry produces an equal but opposite change in $g_{0\nu}$ to restore Ricci flatness, as in the last diagram.

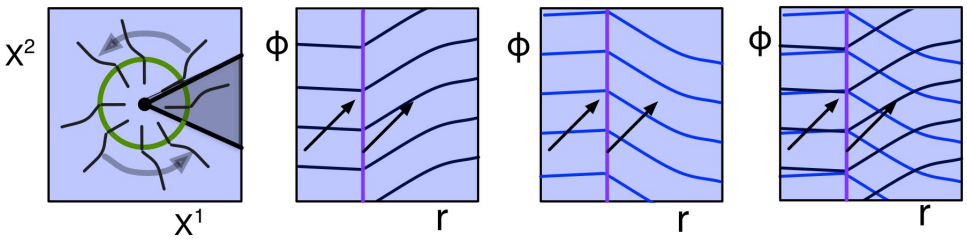

FIG. 10: This figure is similar to Fig. 9 except that it shows the cusp relation for $g_{3\nu}$ rather than $g_{0\nu}$. We recall that the index 3 refers to the ϕ coordinate. We take a slice from the ϕ coordinate as shown in the first diagram. The second diagram shows the lines of constant phase for the waves that circulate around the particle. The third diagram shows the lines of constant A^3. The fourth diagram shows both the lines of constant phase and constant A^3. Crossing fewer black lines decreases the distance because it decreases the distance traveled in x^4 and x^5. Crossing more blue lines increases the effective distance because it increases the change of A^3 coordinate, which increases the distance in $g_{\mu\nu}$. We have these two effects negate each other by having their cusps with opposite orientation, as in the fourth diagram. In this way, we eliminate the cusp in the metric for the component $g_{3\nu}$.

V. FIELDS

A. Electromagnetic field

Calculation of $F^{\mu\nu}$ is complicated by the metric $g_{\mu\nu}$ that depends on ρ. We begin the calculation by starting with a simpler case. We assume a flat 3+1 manifold that has a circular charge current source J^ν on the circle $(r, z, \phi) = (1, 0, \phi)$. Then we assume a field $W^{\mu\nu}$ that is defined on the flat 3+1 manifold such that

$$\partial_\mu W^{\mu\nu} = J^\nu \tag{24}$$

and $W^{\mu\nu}$ goes to zero at infinite distance. The divergence condition implies $\int_{\partial V} W^{\mu\nu} \mathrm{d}A_\mu = \int_V J^\nu \mathrm{d}V$: the integral over the surface of a volume V of the outward facing components of $W^{\mu\nu}$ is equal to the integral over the volume of the source current J^ν (in this equation, $\mathrm{d}A_\mu$ is the outward facing area element). If we change the metric on the flat space so that it has conformal weight ρ (making the metric $\rho^2\bar{\eta}_{\mu\nu}$) then we can modify $W^{\mu\nu}$ to preserve the divergence relation. Specfically, we scale the field to make $Y^{\mu\nu} = (1/\rho)W^{\mu\nu}$. In

two dimensions this would restore the condition $\nabla_\mu Y^{\mu\nu} = J^\nu$ for any conformal change of the metric. In 3+1 dimensions, the axially symmetric case that we are considering happens to also satisfy this relation. The ϕ and t coordinates scale by a factor of ρ due to the conformal factor of the metric, but the Lorentz contraction scales the volume element $\mathrm{d}V$ by a factor of $1/\gamma = 1/\rho^2$. The volume element $\mathrm{d}V$ is therefore unchanged. Because the field is axially symmetric in ϕ, this implies that we retain the desired condition $\nabla_\mu Y^{\mu\nu} = J^\nu$.

The electromagnetic field has a Lagrangian of the form $\int \mathcal{L}\,\mathrm{d}\Phi_M = \int w F^{\alpha\beta}F_{\alpha\beta}\,\mathrm{d}\Phi_M$ on the spacetime manifold. The w term is the quantum branch weight, $w = \rho^4$. From section IV A 3, Ricci flatness requires $\gamma = \rho^2$. The Lorentz-contracted volume is $\mathrm{d}\Phi_M = (1/\gamma)\mathrm{d}t\mathrm{d}V = (1/\rho^2)\mathrm{d}t\mathrm{d}V$. Therefore the Lagrangian is

$$\int \mathcal{L}\,\mathrm{d}\Phi_M = \int (\rho^4/\gamma) F^{\alpha\beta}F_{\alpha\beta}\,\mathrm{d}t\mathrm{d}V = \int \rho^2 F^{\alpha\beta}F_{\alpha\beta}\,\mathrm{d}t\mathrm{d}V = \int \rho F^{\alpha\beta}\rho F_{\alpha\beta}\,\mathrm{d}t\mathrm{d}V \tag{25}$$

With a charge current J^α, the field equation is

$$\nabla_\mu \frac{\partial(\rho F^{\alpha\beta}\rho F_{\alpha\beta})}{\partial(\rho A_\alpha{}^{,\mu})} = \nabla_\mu(\rho F^{\alpha\mu}) = J^\alpha \tag{26}$$

This implies $\rho F^{\mu\nu} \propto Y^{\mu\nu} = (1/\rho)W^{\mu\nu}$, and therefore

$$F^{\mu\nu} \propto (1/\rho^2)W^{\mu\nu} \tag{27}$$

B. Geometric field

The Lagrangian of this theory, including the scalar curvature R, is

$$\mathcal{L} = \rho^4\Big((1/2)F^{\alpha\beta}F_{\alpha\beta} - R\Big) \tag{28}$$

We note that this is scalar curvature R relative to $\bar{\eta}^{\mu\nu}$, and not $\hat{R}$ relative to $g^{\mu\nu}$. A field generated by the R term in the Lagrangian also propagates and has momentum. We showed previously how the electromagnetic field cusp produces a geometric field cusp. In this section we describe the geometric field that results from the geometric field cusp.

When it is necessary to distinguish between the geometric field of gravity and the geometric field that results from the charge cusp, we will refer to the charge-generated field as the geometric charge field. The geometric charge field on the charged $\mathbb{R}^3\#(S^1 \times P^2)$ is distinct from the gravitational field. The source for the gravitational field is the energy-momentum

tensor, which is additive for multiple particles. The source for the geometric charge field is the charge-generated cusp, and it is not additive for multiple particles. Though the fields are distinct, they both arise from the scalar curvature term in the Lagrangian and have some similarities. The gravitational field for a steadily rotating mass has a gravitoelectromagnetic field with components E_g and B_g, analogous to the electric and magnetic fields of electromagnetism. The geometric charge field has analogous components E_{gc} and B_{gc} whose source is the geometric cusp. In the left diagram of Fig. 11 we see a knot on which E_{gc} and B_{gc} are zero. In the right diagram we see a knot on which the fields are non-zero. We compose the fields E_{gc} and B_{gc} into a single field $C^{\mu\nu}$. Using the standard field $W^{\mu\nu}$ from section V A, we write $C^{\mu\nu} \propto (1/\rho^2)W^{\mu\nu}$ (also proportional to the electromagnetic field $F^{\mu\nu} \propto (1/\rho^2)W^{\mu\nu}$). To find the relative magnitudes of the momenta from geometry and electromagnetism, we compare features of the fields.

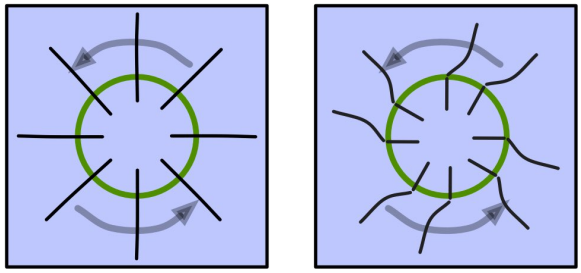

FIG. 11: In the left diagram we take a slice of a neutral $\mathbb{R}^3\#(S^1 \times P^2)$. There are waves circulating around the particle and the lines of constant phase are shown in black. Because the particle is neutral, the phase displacement is zero. If the particle is charged, then Ricci flatness requires that the geometry of the waves negate the cusp corresponding to the electrmagnetic field. This implies that the phase displacement comes to a cusp, as in the diagram on the right. Stretching the geometry in this way requires energy. As the waves circulate around the knot, that geometric energy also contributes to the angular momentum.

In [1] we described how the geometry of the manifold relates to entropy and the Lagrangian. Specifically, the Lagrangian has scalar curvature term $\mathcal{L} = -wR$. We recall from [1] that the manifold M is modeled by an unbranched manifold Φ_M and that stretching Φ_M reduces the geometric entropy of the branches of M. We can use the Lagrangian to find the amount of force and energy that result from that reduction of entropy. In the weak field limit, stretching the manifold Φ_M by an extension x produces results analogous

to Hooke's law with force $F = -kx$ and energy $E = (1/2)kx^2$. To find the energy associated with a particular extension, we therefore need to find the magnitude of the extension x and the analogous spring constant k.

C. Field extension

The geometric field occurs because of waves in the function h that scale the amplitude of the form

$$X(t, \tau, \sigma, \phi) = \Big(t, \tau/(1-\tau), \sigma, \phi, h\tau \sin(2\sigma + \omega t), h\tau \cos(2\sigma + \omega t)\Big) \tag{29}$$

Scaling by h affects the values A^4 and A^5. The derivatives h' at the cusp have the form $A_{4,0}$, $A_{5,0}$, $A^4{}_{,\nu}$, and $A^5{}_{,\nu}$. If we set the derivatives h' so that the metric is Ricci flat at the cusp then, from section IV B, we see that the geometric field derivatives h' have the same magnitude as the electromagnetic field derivatives $A^0{}_{,\nu}$ and $A^3{}_{,\nu}$ at the cusp. However, the effect on the entropy is determined by the amount of geometric extension produced by the derivatives h'. Changing h changes the amplitude of the knot. Changing the amplitude changes the circumference of the $S^1 \times P^2$ at the cusp. In particular, for a fixed ϕ slice, the circumference of the P^2 is $C = 4\pi h$. A change Δh therefore changes the circumference by $\Delta C = 4\pi \Delta h$. The entropy of the geometry is reduced by that effect of stretching the circumference. The energy associated with the derivatives h' is $E = (1/2)k(4\pi h')^2$, which is $16\pi^2$ times larger than the corresponding energy for the electromagnetic field.

D. Degrees of freedom

Both the electromagnetic field and geometric field are derivatives of A^ν. To compare the microstates in electromagnetism and geometry, we compare the number of degrees of freedom that are part of the electromagnetic field and the geometric field. The field $F^{\mu\nu}$ is determined by derivatives in directions parallel to the manifold M. This gives variation of A^ν in 4 directions, for 4 degrees of freedom. There are 5 spacelike directions for geometric effects on entropy that correspond to the field $C^{\mu\nu}$. Therefore, the ratio of degrees of freedom in the geometric field compared to the electromagnetic field is 5/4.

E. Geometric fields summary

A charged particle has an electromagnetic field with a cusp. The electromagnetic field cusp alone does not satisfy Ricci flatness. To make the metric Ricci flat, the geometric field has a cusp with curvature that compensates the curvature of the electromagnetic field cusp. This produces fields E_{gc} and B_{gc} satisfying the same field equations as the electromagnetic fields E and B. The two fields E_{gc} and B_{gc} combine into a single tensor $C^{\mu\nu}$. The relative magnitude of the momentum from $C^{\mu\nu}$ compared to $F^{\mu\nu}$ comes from the relative effect on entropy. The field $C^{\mu\nu}$ has a displacement that is 4π times larger than the corresponding displacement in $F^{\mu\nu}$, which increases the momentum by a factor of $16\pi^2$. The field $C^{\mu\nu}$ has 5 degrees of freedom and $F^{\mu\nu}$ has 4 degrees of freedom. Therefore the geometric field has momentum that is $(5/4)16\pi^2 = 20\pi^2$ times larger than the electromagnetic field momentum.

F. Energy and momentum on the electron

For the electromagnetism Lagrangian $\int \mathcal{L}\,\mathrm{d}\Phi_M = \int (1/\gamma)\mathcal{L}\,\mathrm{d}t\mathrm{d}V = \int (\rho^4/\gamma)F^{\alpha\beta}F_{\alpha\beta}\,\mathrm{d}t\mathrm{d}V$ the energy momentum tensor is

$$T^{\mu\nu} = \Big(\frac{\rho^4}{\gamma}\Big)\Big(- F^{\alpha\mu}F_{\alpha}{}^{\nu} + (1/4)\bar{\eta}^{\mu\nu}F^{\alpha\beta}F_{\alpha\beta}\Big) \tag{30}$$

On an embedded manifold, the term $\bar{\eta}^{\mu\nu}F^{\alpha\beta}F_{\alpha\beta}$ can have momentum if there are transverse waves. The transverse waves have velocity $\bar{\eta}^{0\nu}$ that transports energy of the form $\bar{\eta}^{0\nu}F^{\alpha\beta}F_{\alpha\beta}$. However, Lagrangian optimization implies that the effect on $T^{\mu\nu}$ is equivalent whether the field is of the form $-F^{\alpha\mu}F_{\alpha}{}^{\nu}$ or $\bar{\eta}^{\mu\nu}F^{\alpha\beta}F_{\alpha\beta}$. For that reason we calculate as if all field momentum is of the form $-F^{\alpha\mu}F_{\alpha}{}^{\nu}$. We include the geometric field $C^{\mu\nu}$ and the momentum is

$$T^{0\mu} = -\Big(\frac{\rho^4}{\gamma}\Big)\Big(F^{\alpha\mu}F_{\alpha}{}^{0} + C^{\alpha\mu}C_{\alpha}{}^{0}\Big) \tag{31}$$

where $C^{\alpha\mu}C_{\alpha}{}^{0} = (5/4)16\pi^2F^{\alpha\mu}F_{\alpha}{}^{0}$ and $F^{\mu\nu} \propto (1/\rho^2)W^{\mu\nu}$ and $\gamma = \rho^2$. We use a proportionality constant k_F such that $F^{\mu\nu} = (1/\rho^2)k_F^{1/2}W^{\mu\nu}$. Then total momentum is

$$T^{0\mu} = -(1 + 20\pi^2)(1/\rho^2)k_F W^{\alpha\mu}W_{\alpha}{}^{0} \tag{32}$$

VI. MATHEMATICAL MODEL

The mathematical model is available as a Mathematica™ notebook file on **www.knotphysics.net**. The mathematical model generates the conformal factor ρ and the field $W^{\mu\nu}$ and then integrates the angular momentum $\vec{r} \times \vec{p}$ to get the spin angular momentum S using the formula

$$S = \int rT^{0\mu} \mathrm{d}V = \int r(1 + 20\pi^2)(1/\rho^2) k_F W^{\alpha\mu} W_{\alpha}{}^{0} \mathrm{d}V \tag{33}$$

A. Inputs and calculations

We describe the inputs and calculations done in the Mathematica™ notebook. We use polar coordinates **(r, z, phi)** and toroidal coordinates **(tau, sigma, phi)** for the mathematical model. All calculations are done in the **(r, z)** plane, which is also the **(tau, sigma)** plane, and extended to **phi** by symmetry.

The following is a list of the functions and inputs in the mathematical model. All functions use toroidal coordinate inputs. The vector-valued functions produce vectors that are in toroidal coordinates. Toroidal coordinates are orthogonal, which implies that cross products such as $\vec{E} \times \vec{B}$ do not need angular corrections.

- **radius**: the S^1 radius of the particle. An input. Can be any positive value.
- **charge**: the particle charge. An input. Can be any non-zero value.
- **rco(tau,sigma,phi)**: the value of the r coordinate in cylindrical coordinates. This is necessary to calculate angular momentum $\vec{r} \times \vec{p}$.
- **dVtor(tau,sigma)**: the volume measure dV using toroidal coordinates. This is used to calculate the integral of angular momentum in toroidal coordinates.
- **harmonic(tau,sigma)**: a harmonic function whose source is the circle at tau=∞.
- **rho(tau,sigma)**: the conformal factor ρ of quantum branch weight such that $\rho^4 = w$.
- **DivField(tau,sigma)**: a vector field that has zero curl and has divergence that is zero everywhere except at tau=∞.

- **ScaledDivField(tau,sigma)**: a scaling of DivField so that the divergence is equal to the charge. On flat space, this would be the electric field.
- **StokesCurrent(tau,sigma)**: a function to assist the calculation of CurlField.
- **CurlField(tau,sigma)**: a vector field that has zero divergence and has curl that is zero everywhere except at tau=∞.
- **ScaledCurlField(tau,sigma)**: a scaling of CurlField so that the curl is equal to the current. On flat space, this would be the magnetic field.

We then use **ScaledDivField** and **ScaledCurlField** as components of the flat space field tensor $k_F^{1/2} W^{\mu\nu}$. The product $k_F W^{\alpha\mu} W_\alpha{}^0$ is the cross product of **ScaledDivField** and **ScaledCurlField**. Then the spin angular momentum is $S = \int r(1 + 20\pi^2)(1/\rho^2) k_F W^{\alpha\mu} W_\alpha{}^0 \, \mathrm{d}V$, using the above calculated functions. The inverse fine structure constant estimate is $\alpha^{-1} = (8\pi S)(1/q^2)$.

B. Momentum calculations

The calculation for α^{-1} is approximately $\alpha_{calc}^{-1} = 136.854$, compared to the experimental value $\alpha_{exp}^{-1} = 137.036$. The error is -0.18 and the percent error is 0.13%. The calculation was performed, in part, by comparison of the entropy in electromagnetic fields to the entropy in geometry. That entropy comparison follows from comparing the way that fields affect the microstates of electromagnetism and geometry. However, the microstates that were considered all had flat topology. The microstates associated with virtual fermions were not counted. For example, the electric field affects the microstates of virtual electron/positron pairs by increasing the probability that pair production will put the charged particles in opposite alignment to the field. That reduces the entropy of the particle pairs. To increase the accuracy of the calculation, one would need to develop additional methods of accounting for the effect on entropy from electromagnetic and geometric fields. Comparing those entropic effects would then give a comparison relative to particle charge.

VII. OTHER PARTICLES

The derivation in this paper showed the relationship between Planck's constant and the charge of the electron. The derivation used the topology of the electron to show how Lagrangian optimization of the geometry and fields produced a fixed ratio between spin angular momentum and the square of the charge. To perform this same derivation on a charged lepton of another generation, one would follow almost exactly the same procedure. A charged lepton has topology $\mathbb{R}^3\#(S^1 \times P^2)_n$ for some $n \geq 0$. The spin angular momentum is a constant $\hbar/2$, resulting from the expected amount of entropy for a single degree of freedom. We know from the calculation that changing the radius of the knot does not affect the relationship between charge and spin angular momentum. We conclude that the expected charge is the same for any charged lepton.

When deriving the charge on hadrons there are additional complications. When we Ricci flatten a particle that has multiple linked $\mathbb{R}^3\#(S^1 \times P^2)$, we find that the geometry has become more complicated than the leptonic case. Again, the Weyl metric characterizes every axially symmetric solution. We expect that the hadron can still be described with a Weyl metric $g_{\mu\nu}$. However, that metric on the hadron must be consistent with the more complicated particle topology. For example, the two dimensional description of a baryon would imply using the Gauss-Bonnet theorem on $\mathbb{R}^2\#P^2\#P^2\#P^2$. For a hadron, it may be necessary to use an electromagnetic field just to achieve Ricci flatness, which would explain why there are no uncharged quarks. The fact that baryons can have charge magnitude 2 is also an indication that there is a greater variety of configurations for quarks than are possible for leptons.

VIII. CONCLUSION

We used the geometry of a charged lepton to derive its spin angular momentum as a function of the charge. Other factors, such as particle radius, have no net effect on the spin angular momentum. We therefore conclude that there is a fixed relationship between the spin angular momentum and the charge. The spin angular momentum is fixed at $\hbar/2$, therefore the charge must also be fixed. The relationship between Planck's constant and electron charge is expressed using the fine structure constant, which we derived here. The

derived result of $\alpha^{-1} = 136.85$ is different from the measured result $\alpha_{\text{exp}}^{-1} = 137.04$ by 0.18, which is 0.13%. Including additional Feynman diagrams in the calculation may reduce the error.

---

[1] C. Ellgen **www.knotphysics.net** Physics on a Branched Knotted Spacetime Manifold

[2] L.A. D'Afonseca, P.S. Letelier, S.R. Oliveira Geodesics around Weyl-Bach's Ring Solution (2008) http://arxiv.org/pdf/gr-qc/0507033v2.pdf

[3] J. Besse, Springer **Einstein Manifolds**, (1987).